



Synthesis and characterization of nanoparticles from neem leaves and banana peels: a green prospect for dye degradation in wastewater

Ahana Sengupta¹ · Angana Sarkar¹

Accepted: 8 April 2021 / Published online: 27 April 2021

© The Author(s), under exclusive licence to Springer Science+Business Media, LLC, part of Springer Nature 2021

Abstract

Nanoparticles have excellent catalytic, adsorptive, and reactive properties, which led to their application for wastewater treatment. The current study focuses on silver nanoparticle synthesis using neem leaf and banana peel extract and its application as an antimicrobial and dye degrading agent for wastewater treatment. The use of these extracts led to a rapid, simple, and environment-friendly method for the biosynthesis of silver nanoparticles (AgNPs). UV-Vis spectroscopy showed absorption bands at 473 and 423 nm for AgNPs synthesized from neem leaf and banana peel extracts, respectively. The AgNPs were further characterized using XRD, FTIR, ESEM, EDX, and DLS methods. XRD data confirmed the crystalline nature of the synthesized AgNPs. ESEM images revealed the synthesized nanoparticles were spherical. From DLS analysis the average diameter of the AgNPs was found to be 168.7 nm from banana peel and 206.4 nm from neem leaf extract. Antibacterial activity of synthesized nanoparticles at 0.025 mg/ml concentration was tested against *Escherichia coli* (*E.coli*), *Bacillus subtilis* (*B.subtilis*), *Staphylococcus aureus* (*S.aureus*), and *Klebsiella* sp. using disk diffusion method and the zone of inhibitions observed were 10–13, 3–4, 2–3, and 1–3 mm respectively. 99% degradation of model dye malachite green was observed using banana peels-derived nanoparticles at a concentration of 0.06 mg/ml within 4.5 h. This study provides an eco-friendly and economic approach to AgNP synthesis and its potential application in the removal of hazardous dye from wastewater.

Keywords Banana peels · Neem leaf · Green synthesis · Eco-friendly · Silver · Antibacterial · Nanoparticle · Wastewater

Introduction

Urbanization and rapid growth of different industries have led to environmental pollution which has impacted ecology as well as human health. Water pollution has become a cause of major concern worldwide. It mainly arises due to the discharge of the untreated effluents into the water bodies from different industries. Pollution due to the discharge of a high amount of non-biodegradable organic compounds such

as dyes plays a wicked role in enhancing worldwide pollution. Dyes are known to be synthetic organic compounds and when they are dissolved in water they are known to cause major water pollution all over the world. It is very critical to treat the dye-containing wastewater before it is being discharged into the water bodies (Samanta et al. 2016). Degradation of dyes using physical, chemical, and biological processes has been reported but it has been observed that these processes often are ineffective as it is time-consuming and also quite a large amount of effluent is generated. Studies have been performed to utilize metal nanoparticles known to possess novel electronic and physicochemical properties for dye degradation (Jyoti and Singh 2016). Different studies have shown that these azo dyes have the potential of causing different diseases. And also due to the presence of the chromophoric group in dyes, it can impart color which can not only hamper the aesthetics but also prevents penetration of sunlight and which in turn negatively impacts the aquatic ecosystem. One of the

Supplementary information The online version contains supplementary material available at <https://doi.org/10.1007/s10646-021-02414-5>.

✉ Angana Sarkar
sarkara@nitrkl.ac.in

¹ Department of Biotechnology and Medical Engineering, National Institute of Technology, Rourkela, Odisha, India

approaches for the degradation of dye is catalytic or photocatalytic degradation using metallic nanoparticles. The application of nanotechnology for wastewater treatment includes the use of the synthesized nanoparticles as an adsorbent or as a catalyst. The field of nanotechnology is growing rapidly and is proving to be an active area of research. Due to the vast variety of applications of nanomaterials in diverse fields, for example, optoelectronics, biotechnology, biomedicine, and others the need for nanoparticle synthesis is increasing day by day (Bankar et al. 2010; Gan et al. 2018; Vidhu and Philip 2014). For nanoparticle synthesis different physical and chemical processes are followed but these methods have their disadvantages (Yurtluk et al. 2018). Thus now processes are required which will be nontoxic, eco-friendly, and clean. For these reasons, biological processes are now being explored for nanoparticle synthesis (Herlekar et al. 2014; Attar and Altikatoglu Yapaoz 2018; Joanna et al. 2018). Green synthesis of a metal nanoparticle is considered advantageous as in this process no hazardous materials are involved. Green synthesis involves the synthesis of nanoparticles via using fungi, bacteria, plants, and animal biomass (Wei et al. 2014). Synthesis of metal nanoparticles using plants is considered better than microbial synthesis, extracellular synthesis of nanoparticles can be done in the plant-mediated system. And also via this method, large-scale synthesis can be done (Mariselvam et al. 2014). AgNP's biosynthesis has been done using different parts of a plant and is shown in Table 1. Various studies have reported that AgNPs act as a good catalyst in dye reduction reactions. Agnihotri et al. (2018) utilized pineapple waste-derived AgNPs for methylene blue degradation and reported a dye removal percentage of 98.04. AgNPs produced from *Cordia dichotoma* leaf extract were used for congo red and methylene blue degradation and they observed complete degradation of congo red within 20 mins and in the case of methylene blue, after 6 h there was a notable decrease in absorption peak which denotes that significant amount of dye was degraded (Kumari et al. 2016). Using silver and gold nanoparticles which were produced from *Mussaenda glabrata* catalytic degradation of rhodamine B and methyl orange dyes were observed and complete removal of dyes was noticed within 10 mins. (Francis et al. 2017). AgNPs synthesized from *Hydrocotyle asiatica* showed 94 and 9.6%, methylene blue and malachite removal percentage respectively under photocatalytic conditions (Devi et al. 2016). In this study degradation of model dye malachite green has been observed. Malachite green a synthetic dye is used in different industries for the production of inks and paints and also in paper, leather, and silk dyeing. And when malachite green is present in the discharged effluent it poses a great threat to the aquatic ecosystem. Thus removal of this dye before its release is

Table 1 Different plants from which silver nanoparticles have been synthesized

Sl no.	Plant	Part of plant	Size and shape of synthesized nanoparticles	Reference
1.	<i>Alternanthera dentate</i>	Leaf extract	50–100 nm Spherical	(Nakkala et al. 2014)
2.	Aloe vera	Leaf extract	50–350 nm Spherical and triangular	(Chandran et al. 2006)
3.	<i>Musa paradisiaca</i>	Peel	23.7 nm Spherical	(Ibrahim 2015)
4.	<i>Ocimum sanctum</i>	Leaf extract	3–20 nm Spherical	(Mallikarjuna et al. 2011)
5.	<i>Ceratonia siliqua</i>	Leaf extract	5–40 nm Spherical	(Awwad et al. 2013)
6.	<i>Olea europaea</i>	Leaf extract	20–25 nm Spherical	(Khalil et al. 2014)
7.	<i>Musa balbisiana, Azadirachta indica and Ocimum tenuiflorum</i>	Leaf extracts	200 nm Spherical, triangular, and cuboidal	(Banerjee et al. 2014)
8.	<i>Eucalyptus hybrida</i>	Peel	50–150 nm Spherical	(Dubey et al. 2009)
9.	<i>Argemone maxicana</i>	Leaf extract	20 nm Cubic and hexagonal	(Singh et al. 2010)
10.	Pomegranate	Peel	5–50 nm	(Shanmugavadivu et al. 2014)
11.	<i>Citrus sinensis</i>	Peel	35 ± 2 nm Spherical	(Kaviya et al. 2011)
12.	<i>Punica granatum</i>	Peel	30 nm Spherical	(Edison and Sethuraman 2013)
13.	<i>Azadirachta indica</i>	Leaf extract	34 nm Spherical	(Hussein et al. 2019)
14.	<i>Syzygium cumini</i>	Leaf and seed extract	30 nm and 92 nm Spherical	(Kumar et al. 2010)

very critical (Hameed and Lee 2009; Du et al. 2011). Devi et al. (2016) study pointed out three plausible causes behind dye degradation. The first reason can be by either reduction or by an increase in pH, the dye may get transformed to its leuco form, the second being the large surface area of nanoparticles can lead to adsorption of dye which will lead to its removal. And the third reason which also confirms our study is that due to the phenomenon of surface plasmon resonance the electrons which are generated can lead to the degradation of dye on the surface of the nanoparticles. In our study, we observed that the synthesized nanoparticles were negatively charged which can lead to the attraction

and adsorption of the cationic dye over the surface of the nanoparticles and eventually the degradation of dye by the excited electrons. AgNPs are also known to have antimicrobial properties which can be utilized for wastewater treatment. AgNPs reportedly have an inhibitory effect on aerobic and anaerobic microbial populations present in sludge. These nanoparticles get absorbed on the bacterial cell wall, disrupt the permeability of the membrane, and ultimately lead to cell lysis and death (Esakkimuthu et al. 2014). In the current work, nanoparticles were biosynthesized from neem leaf and banana peel and then were characterized using UV-Visible spectra, FTIR, ESEM, EDX, DLS, and XRD. Antibacterial activity of the AgNPs was tested against gram-negative bacteria (*Escherichia coli* and *Klebsiella* sp.) and gram-positive bacteria (*Bacillus subtilis* and *Staphylococcus aureus*). And photocatalytic degradation of malachite green dye was studied. This study provides a potential strategy for the treatment of wastewater.

Materials and methods

Preparation of extract from leaves of *Azadirachta indica* (neem) and peels of *Musa* (banana)

Fresh neem leaves were collected from the NIT Rourkela campus area (22°15'20.5"N, 84°54'03.0"E). The leaves at first were cleaned with tap water to remove dirt and then were cleaned with distilled water twice. The washed leaves were then cut into small pieces using sterile scissors. In 200 ml of distilled water 40 g, chopped leaves were boiled at 60–70 °C for 45 mins. Using filter paper (Whatman no. 1) the solution was filtered and was stored at 4 °C. The collected banana peels were washed under tap water and then washed with distilled water twice. Washed banana peels were chopped into small pieces with sterile scissors. 100 g of banana peel was boiled at 60–70 °C for 1 h. Using filter paper the solution was filtered and was stored at 4 °C.

Biosynthesis and purification of silver nanoparticle

Silver nanoparticle biosynthesis was done using both neem leaf and banana peel extract. Neem leaf extract (reducing agent) and silver nitrate solution (1 mM) were mixed in a 1:4 (v/v) ratio. The solution was kept at room temperature and within a particular time change of color to brown was observed which is shown in Supplementary Fig. 1. Banana peel extract and silver nitrate solution (1 mM) were mixed in 1:4 (v/v) ratios. And after heating the solution at 70–80 °C a visual color change to brown was observed and is shown in Supplementary Fig. 1. Both the reactions were performed under static conditions. To reduce the photo-activation of

silver ions both the experiments were performed in dark conditions. The change of color to brown indicated the silver ions reduction (Ahmad et al. 2003). The colloidal solutions containing the synthesized nanoparticles were centrifuged at 7000 rpm for 20 mins after centrifugation the pellet was washed twice with double-distilled water. The pellets obtained were dried overnight at 60–65 °C.

Characterization of silver nanoparticles

UV-Vis spectrophotometer

The reduction of the silver ions by neem leaves and banana peel extract and subsequent AgNP synthesis was observed by the UV-Vis spectrophotometer. The reaction mixtures were scanned in the 200–800 nm range (Ahmad et al. 2003).

Fourier transform infrared spectroscopy (FTIR)

Different functional groups present within the extract and the synthesized nanoparticles were determined by FTIR analysis using α E Fourier Transform InfraRed Spectrophotometer, Bruker, USA. A dried powder sample was used for the analysis. Dried powder of control sample i.e. dried neem leaves and banana peels, and test sample i.e. the AgNPs were used for analysis. The samples were scanned in the 4000–400 cm^{-1} range (Banerjee et al. 2014).

Environmental scanning electron microscope (ESEM)

ESEM (JSM-6480LV, JEOL, USA) study was done to visualize the structure of the biosynthesized nanoparticles. A solution containing silver nanoparticles was cast on glass slides and then was coated with gold for ESEM analysis (Shanmugavadivu et al. 2014).

Energy-dispersive X-ray spectroscopy (EDX)

For elemental analysis of the synthesized nanoparticles, EDX (JSM-5800, JEOL) was performed. The sample preparation was similar to ESEM. Here also samples were loaded onto glass slides and were coated with gold (Banerjee et al. 2014).

X-ray diffraction spectroscopy (XRD)

XRD analysis (Philips PAN analytical, Netherland) was done for the determination of the nanoparticle's crystalline nature. The dried powdered sample was used in the study. The nanoparticles were studied with $\text{CuK}\alpha$ radiation with 40 kV and 40 mA of voltage and current respectively. At a 2θ angle from 20° to 80° the diffracted intensities were recorded (Ibrahim 2015).

Particle size analysis and zeta potential measurement

The hydrodynamic diameter and surface charge of the silver nanoparticle synthesized from neem leaf extract and banana peel extract were performed using a dynamic light scattering method (ZETA sizer Nano series, Malvern instrument Nano Zs). The colloidal solution of the synthesized AgNPs was used (Varadavenkatesan et al. 2019).

Antibacterial activity assay

Antimicrobial activity of the AgNPs was tested against *E. coli*, *B.subtilis*, *S. aureus*, and *Klebsiella* sp. 200 µl of bacterial culture were spread on LB plates. To determine the antibacterial activity disk diffusion method was utilized; disks were soaked in 40 µl of silver nanoparticle solution and then were dried in a sterile condition and placed on the plates. Disks of antibiotic tetracycline were taken as positive control and disks soaked with distilled water were used as negative control and also disks soaked with neem leaf extract and banana peel extract to observe their effect were taken. The inhibition zone was observed after overnight incubation.

Minimum inhibitory concentration (MIC) determinations

MIC values of AgNPs synthesized from neem leaf and banana peel extract was determined. AgNPs at different concentration such as 0.062, 0.124, 0.186, 0.25, and 0.312 mg/ml were added to 100 ml of LB broth inoculated with 0.1 ml of *E.coli*, *B.subtilis*, *S.aureus*, and *Klebsiella* sp. culture. AgNPs at different concentrations were added to the flasks and were incubated overnight at 35 °C at 200 rpm. Absorbance was taken at 600 nm. The concentration which gives the lowest absorbance indicates MIC of AgNPs for that organism (Ahmad et al. 2003; Rautela et al. 2019).

Photocatalytic degradation of dye

Degradation of malachite green was studied using banana peel-derived green AgNPs nanoparticles. A 30 ppm stock solution of Malachite green was prepared. Varying concentration of AgNPs (0.01–0.06 mg/ml) were added to the dye solution. A 3 ml test solution was prepared and mixed thoroughly by drawing 2.8 ml from a stock solution of dye and 0.2 ml from AgNP solution of different concentrations, and these samples were placed under sunlight. A control sample containing only the dye solution was also placed under sunlight. Dye degradation was observed under sunlight for 4.5 h. Using UV-Vis spectrophotometer samples were scanned in the 400–800 nm range (Lakshmi et al. 2016). The standard curve for malachite green dye was

plotted. Percentage degradation was calculated using Eq. (1)

$$\% \text{ Degradation} = (C_0 - C) / C_0 * 100 \quad (1)$$

[C_0 = Initial concentration, C = Final concentration]

Statistical analysis

The minimum inhibitory concentration analysis of AgNPs against *E.coli*, *B.subtilis*, *S. aureus*, and *Klebsiella* sp. culture was performed in three replicates. The mean and standard deviation from the MIC data were calculated.

Results and discussion

UV-Vis spectroscopic analysis of synthesized nanoparticles

Nanoparticles have an optical property that depends upon their shape and size. The biosynthesis of AgNPs was confirmed by a change in color. A color change from colorless to brown indicates silver ions were being reduced to AgNPs by neem leaf and banana peel extract. It is reported because of surface plasmon vibration the brown color develops, which corresponds to silver nanoparticle synthesis (Varadavenkatesan et al. 2019; Ahmad et al. 2003). To monitor the bioreduction of Ag^+ and the formation of AgNPs from an extract of neem leaf and banana peel UV-Vis spectroscopy analysis was performed. From the spectroscopy result, it was observed that the absorption maxima were found to be 473 nm and 423 nm for silver nanoparticles from neem leaf extract and banana peel extract respectively, the absorption spectra are shown in Fig. 1. The biosynthesis of AgNPs using *Ocimum sanctum* leaf extract was reported in a study and they observed a sharp band at 436 nm (Mallikarjuna et al. 2011), silver nanoparticle synthesized using carob leaf extract produced SPR band near 420 nm (Awwad et al. 2013), silver nanoparticle synthesized using citrus peels showed SPR band at 445 nm at room temperature (Shanmugavadivu et al. 2014). The λ_{max} values for silver nanoparticles are reported to be in the visible region between 400–500 nm (Tripathi et al. 2009). In our study, the absorption bands were observed within this region and it correlates with previous reports.

Characterization of the synthesized nanoparticles

Fourier transform infrared spectroscopy analysis

FTIR analysis of neem leaf extract and banana peel extract before and after the addition of salts were performed. FTIR analyses were done to observe the presence of different chemical groups in the extract and their function in the

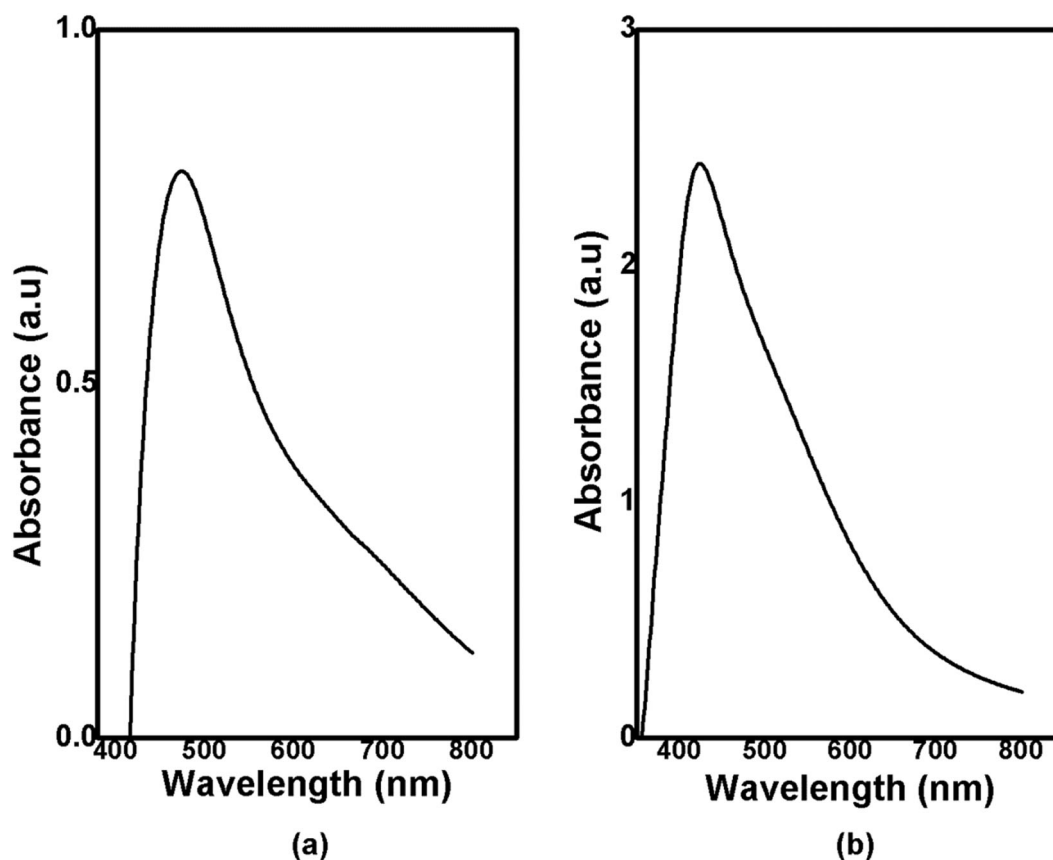


Fig. 1 a Absorption spectrum of AgNP synthesized from neem extract. b Absorption spectrum of AgNP synthesized from banana peel extract

biosynthesis of AgNPs. On performing FTIR analysis of neem leaf extract, shown in Fig. 2 different bands were observed. The bands arising at the 3273.2, 2928.4, 2859, 1716.2, 1601.9, 1018.3 cm^{-1} can be assigned to the stretching vibrations of O-H of alcohol, N-H of amine, C-H of alkane, C=O of carboxylic acid, C=C of alkene, C-O stretching of alcohol. After the reaction of silver nitrate with neem leaf shift in the peak was observed from 1601.9 to 1523.8, 1018.3 to 1026.4 cm^{-1} . FTIR analysis of banana peel extract showed bands at the 3279.4, 2926.3, 1559, 1383.5, 1026.4 cm^{-1} which can be due to stretching vibration of O-H of alcohol, C-H of alkane, C=C of alkene, C-H of aldehyde, C-O stretching of alcohol respectively. On the reaction of silver nitrate with banana peel extract the following shift in peaks was observed 3279.4 to 3273.2, 1559–1603.9, 1383.5 to 1314.2, 1026.4 to 1004 cm^{-1} . The FTIR analysis of silver nanoparticles synthesized using banana, neem, and tulsi showed peaks that correspond to germinal methyls, ether linkages, alkyne groups, and these bands are mainly responsible for terpenoids, flavonoids like compounds. And thus maybe these compounds were involved in the biosynthesis of silver nanoparticles (Banerjee et al. 2014). In another study, the nanoparticles were

synthesized using banana peels and the FTIR analysis of the control i.e. the banana peel showed various bands that correspond to different functional groups. The groups observed were amine, alcohol, alkanes, ester, carboxylic acid, amides, and aliphatic amines. On FTIR analysis of the test sample i.e. the synthesized nanoparticle, a shift in the peaks was observed and it was reported that groups like amide, hydroxyl, and carboxyl maybe were involved in nanoparticle synthesis (Ibrahim 2015). Another study conducted using banana peels for the biosynthesis of AgNPs, from their FTIR analysis they reported that peaks corresponding to N-H stretching, C-O stretching in carboxyl groups, C-N bending in amide group, aliphatic and aromatic compounds, methylene, and methyl groups were observed. It was observed that for all the compounds there was a shift in the peaks in the test sample (i.e. extract of banana peel and silver nitrate solution) which indicates the involvement of these groups in the nanoparticle synthesis (Bankar et al. 2010). FTIR spectra of neem leaf broth and synthesized AgNPs were reported in a study. From the FTIR spectra, they observed peaks that indicate germinal methyl group (1380 cm^{-1}), C=C group (1635 cm^{-1}), and O-H stretching (3389 cm^{-1}). The presence of terpenoids in neem leaf

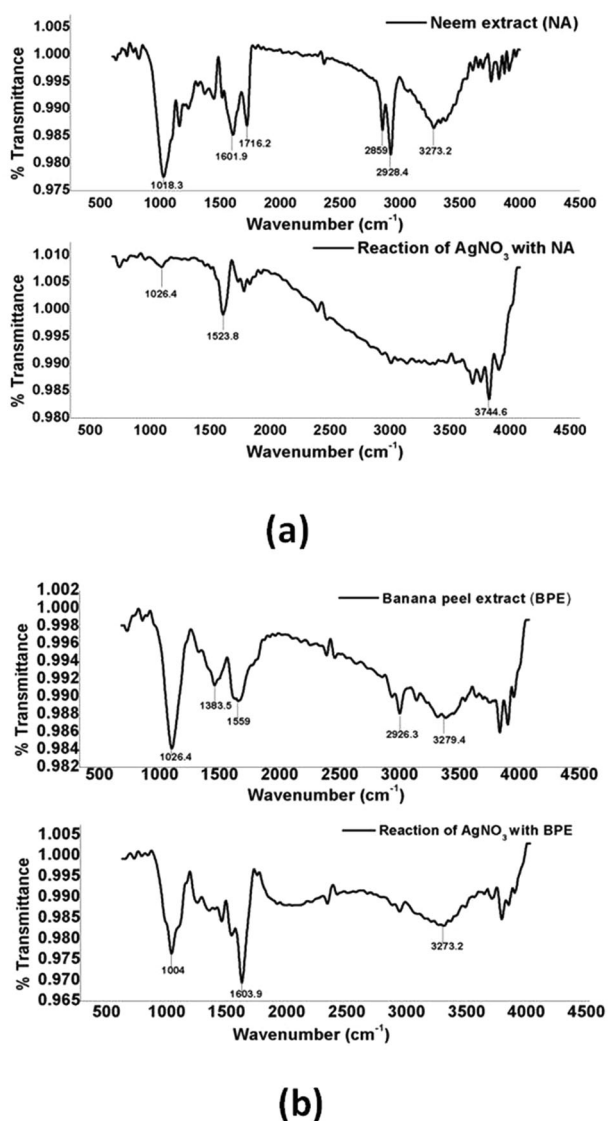


Fig. 2 FTIR graphs of (a) neem leaf extract before and after treatment with AgNO₃ salt; (b) banana peel extract before and after treatment with AgNO₃ salt

extract can be inferred due to the presence of these peaks (Verma and Mehata 2016). From FTIR analysis of our test samples, we observed bands for groups like alcohol, amine, alkane, carboxylic acid, alkene, aldehyde, and amine. And it can be said that these functional groups might be responsible for the synthesis of AgNPs.

Environmental scanning electron microscopy (ESEM) analysis

ESEM analysis provided information regarding nanoparticle structure. The biosynthesized nanoparticles were observed to be spherical. Figure 3 represents the ESEM images of the biosynthesized nanoparticles. SEM images of

AgNPs synthesized from carob leaf extract showed that they were spherical and their size ranges from 5–40 nm (Awwad et al. 2013). Peels of pomegranate were utilized for nanoparticle synthesis in a study and SEM analysis revealed spherical nanoparticles and with size in 5–50 nm range (Shanmugavadivu et al. 2014). In another study, SEM images of silver nanoparticles produced from leaves of banana, neem, and tulsi revealed spherical, triangular, and cuboidal shapes respectively (Banerjee et al. 2014). Different shapes and sizes of AgNPs obtained from different plant parts are also given in Table 1.

Energy-dispersive X-ray spectroscopy (EDX) analysis

EDX analysis data provided the elemental analysis of the synthesized nanoparticles. Figure 3 shows the EDX spectrum of the AgNPs. A silver signal was seen in the EDX spectrum along with peaks of oxygen and carbon in both cases. EDX analysis in a study reported a peak at 3 keV which confirmed silver nanoparticle formation from banana peel extract (Ibrahim 2015). A peak at 3 keV from EDX analysis of silver nanoparticles was also reported in other studies using banana peel extract (Bankar et al. 2010), neem extract (Tripathi et al. 2009), and seed extract of teak (Rautela et al. 2019) as the reducing agent. A peak observed at 3 keV usually denotes metallic AgNPs. EDX analysis of AgNPs from different leaf extracts, along with a distinct silver peak also showed oxygen and carbon peaks (Banerjee et al. 2014). From EDX analysis in the current study carbon and oxygen peaks were observed, the reason behind the peaks might be due to biomolecules present on the nanoparticle surface.

X-ray diffraction analysis

XRD was done to determine the crystalline nature of the nanoparticles. Dried powder of the nanoparticles obtained from the banana peel and neem leaf extract was used for the analysis. At a 2θ angle from 20° to 80° diffracted intensities were recorded. From the results of XRD analysis, it can be said that the AgNPs which were biosynthesized using neem leaf extract and banana peel extract was crystalline. Diffraction peaks at 37.68° , 44.62° , 51.74° , 76.65° and 37.64° , 44.54° , 51.9° , 76.54° in the 2θ range between 20° – 80° [the diffraction peaks were assigned to the (111), (200), (220) and (311) planes of a face-centered cubic lattice of silver] were observed after reaction of neem leaf extract with silver nitrate and banana peel extract with silver nitrate respectively, the XRD spectra is shown in Fig. 3. The results obtained correspond with earlier reports on silver nanoparticles synthesized from banana peel extract (Kokila et al. 2015) and neem leaf extracts (Chandran et al. 2006; Ibrahim 2015; Tripathi et al. 2009).

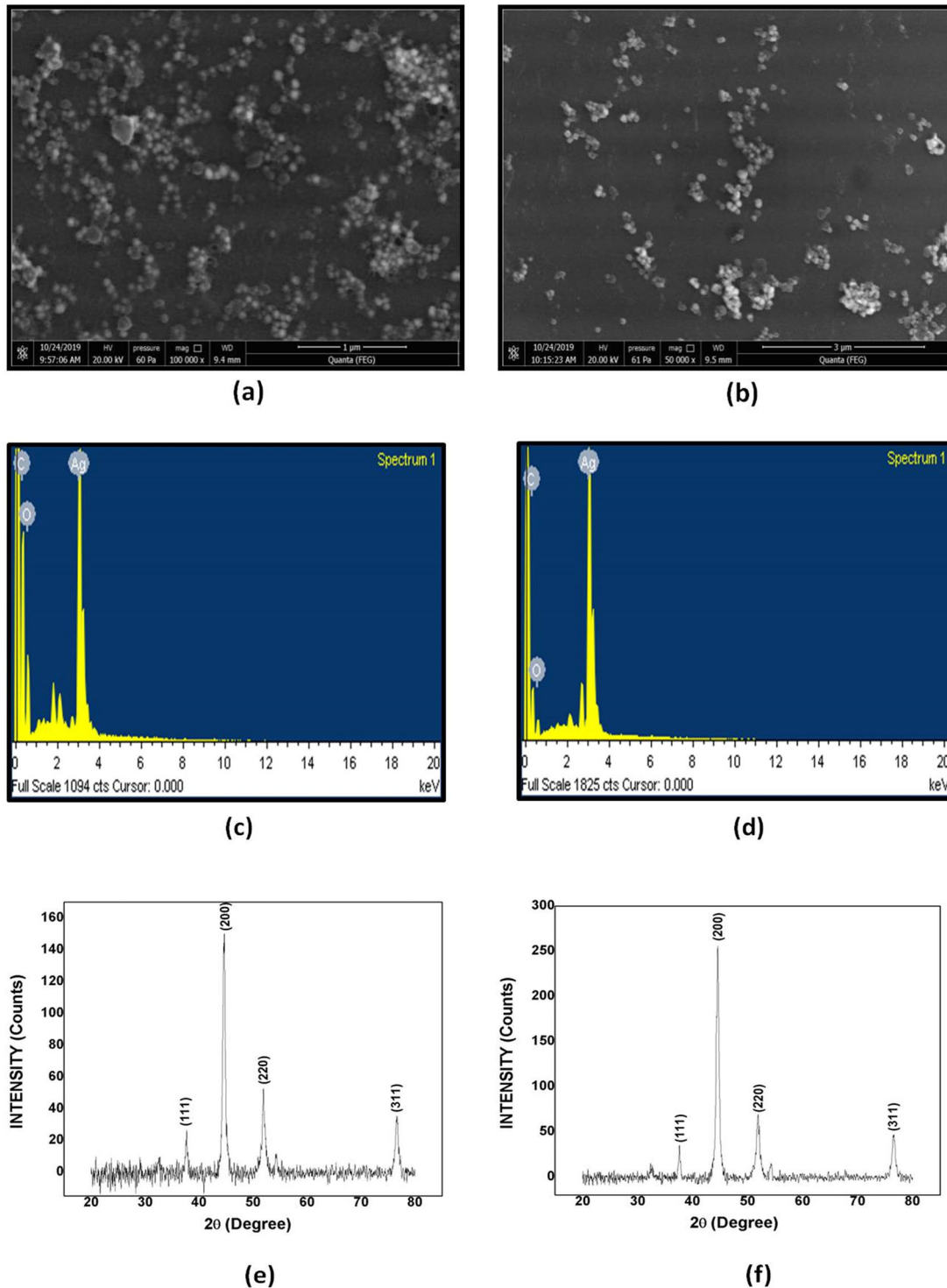


Fig. 3 ESEM image of silver nanoparticle synthesized from (a) neem leaf extract; (b) banana peel extract, EDX spectrum of silver nanoparticle synthesized from (c) neem leaf extract; (d) banana peel extract,

XRD analysis of silver nanoparticle synthesized from (e) neem leaf extract; (f) banana peel extract

Particle size analysis and Zeta potential measurement

The average particle size of the nanoparticles biosynthesized from banana peel was found to be 168.7 nm with a

PDI (Polydispersity index) of 0.394. The zeta potential value was -27 mV. And that from neem leaf extract was found to be 206.4 nm with a PDI (Polydispersity index) of 0.312. In this case, the zeta potential value was -32.7 mV

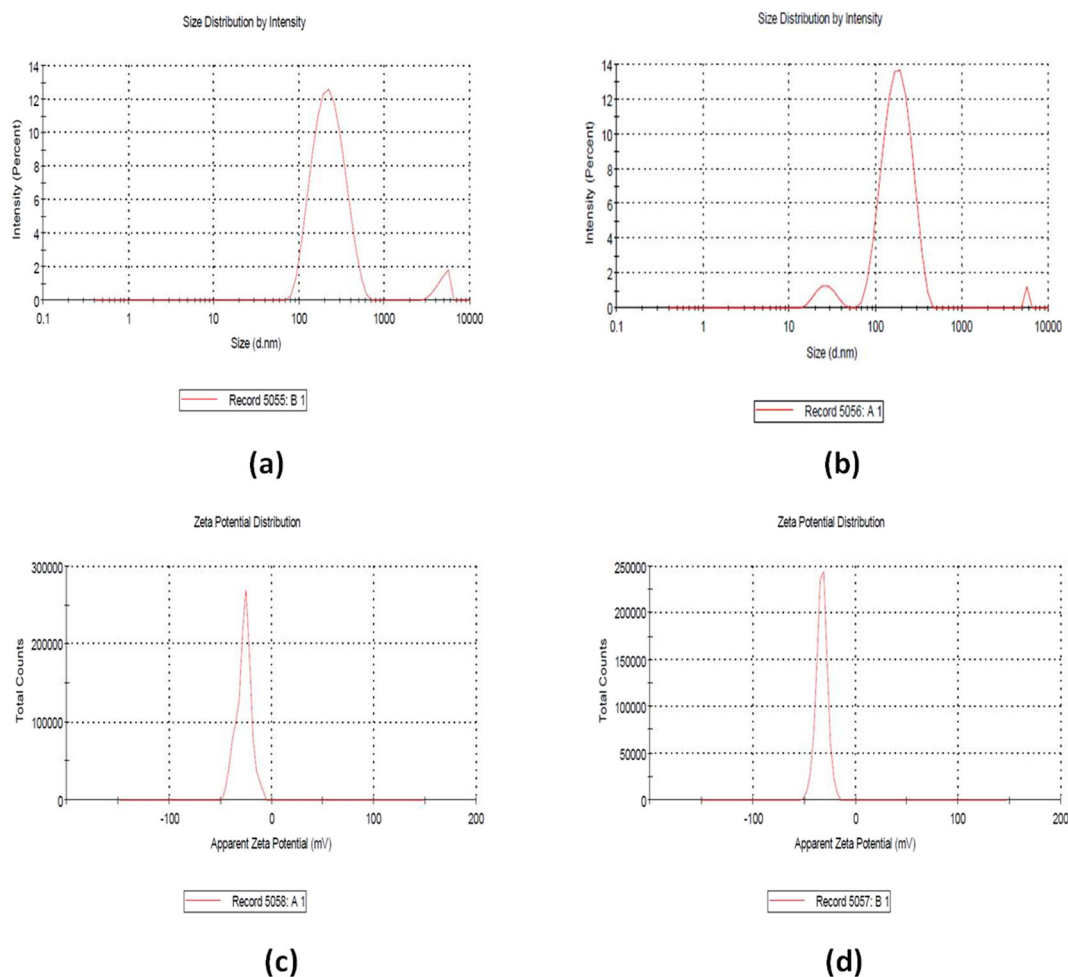


Fig. 4 Particle size distribution of AgNP from (a) Banana peel extract, (b) Neem leaf extract; Zeta potential value of AgNP from (c) Banana peel extract, (d) Neem leaf extract

Table 2 Antimicrobial activity of silver nanoparticles (AgNPs)

Microorganism	Diameter of zone of inhibition (mm)	
	AgNPs from Neem extract	AgNPs from Banana extract
<i>E.coli</i>	13	10
<i>B.subtilis</i>	4	3
<i>S.aureus</i>	2	3
<i>Klebseilla</i>	1	3

(Fig. 4). Particle diameter obtained from DLS analysis appears larger as it represents the hydrodynamic diameter which includes not only the particle diameter but also other molecules or ions attached to it (Varadavenkatesan et al. 2019; Ahmad et al. 2003). A study reported the size of the AgNPs to be 297 nm which was synthesized from banana peel extract (Kokila et al. 2015). It was reported that the PDI value of a nanoparticle system when less than 0.1 is

considered to be highly monodispersed, and when the value is more than 0.4 or in the range 0.1–0.4 it represents highly polydispersed and moderately dispersed distribution respectively (Verma and Mehata 2016; Varadavenkatesan et al. 2019). In our study in both cases, the PDI value is less than 0.4 which indicates moderate dispersity. The most stable zeta potential value is reported to be around ± 30 mV for most nanosuspensions (Ahmad et al. 2003), the zeta potential value obtained from our experiment falls in this range.

Antibacterial assay

Silver nanoparticles (AgNPs) have bactericidal activities against gram-positive and gram-negative bacteria. In our current work, it was seen that the AgNPs at 0.025 mg/ml concentration, the diameter of inhibition zone against *E.coli* was found to be 10–13 mm, 3–4 mm against *B.subtilis*, 2–3 mm against *S.aureus*, and 1–3 mm against *Klebsiella* sp.

(Supplementary Fig. 2). Disk soaked with banana peel extract and neem extract at 0.025 mg/ml concentration was used to observe the antibacterial activity. The zone of inhibition was observed only in the case of disk soaked with neem leaf extract. The diameter of the inhibition zone using neem leaf extract against *E.coli* was found to be less than 4 mm and in the case of *B.subtilis*, *S.aureus*, and *Klebsiella sp.* it was found to be less than 1 mm. This indicated that the silver nanoparticles obtained from the extracts have more antibacterial activity. In Table 2 the diameter of the zone of inhibitions is given. The mechanism behind the antibacterial activity of AgNPs is still not clear. There are different concepts behind the mechanism. One of the mechanisms can be that AgNPs attach to the cell wall of bacteria and consequently penetrates it and causes membrane damage which ultimately leads to leakage of cellular contents and death. The other concept is that AgNPs releases Ag^+ ions, as evidenced in different cases, and these Ag^+ ions when released react with the sulfhydryl groups present in the proteins and enzymes and these might be the reason behind the antibacterial action of Ag^+ ions (Rautela et al. 2019). From antibacterial assay, it was observed that the activity of AgNPs against *E.coli* was higher than *B.Subtilis*, *S.aureus*, and *Klebsiella sp.*

Minimum Inhibitory concentration analysis

The concentration which gives the lowest absorbance indicates MIC of AgNPs for that organism (Ibrahim 2015; Ahmed et al. 2016). OD of the bacterial culture treated with AgNPs was taken at 600 nm using UV-Vis spectra. Graphs were plotted against the concentration of AgNPs synthesized from neem leaf extract (NE) and banana peel extract (BPE) and optical density for the microorganisms tested (Fig. 5). For the microorganisms i.e *E.coli*, *B.subtilis*, and *S. aureus*, at 0.25 mg/ml AgNP (from NE and BPE) concentration, growth was not observed. Thus 0.25 mg/ml was the concentration of AgNP which can inhibit bacterial growth. In the case of *Klebsiella sp.* the MIC value was observed to be 0.312 mg/ml. Loo et al. 2018 reported the minimum inhibitory concentration of AgNPs against *Klebsiella pneumoniae*, *Escherichia coli*, *Salmonella Enteritidis*, and *Salmonella Typhimurium* to be 3.9, 7.8, 3.9, and 3.9 $\mu\text{g/ml}$. AgNPs synthesized from ginger and onion extract showed a minimum inhibitory concentration value of 100 $\mu\text{g/ml}$ against *Staphylococcus aureus* and *Klebsiella pneumoniae* as reported by Hussein et al. (2019). Anti-microbial activity of AgNPs biosynthesized from seed extract of teak against *Staphylococcus aureus*, *Bacillus cereus*, and *Escherichia coli* were determined. It was reported that silver nanoparticles at a concentration of 5.2, 2.0, and 2.6 $\mu\text{g/ml}$ inhibit *Bacillus cereus*, *Escherichia coli*, and *Staphylococcus aureus* respectively (Ahmad and

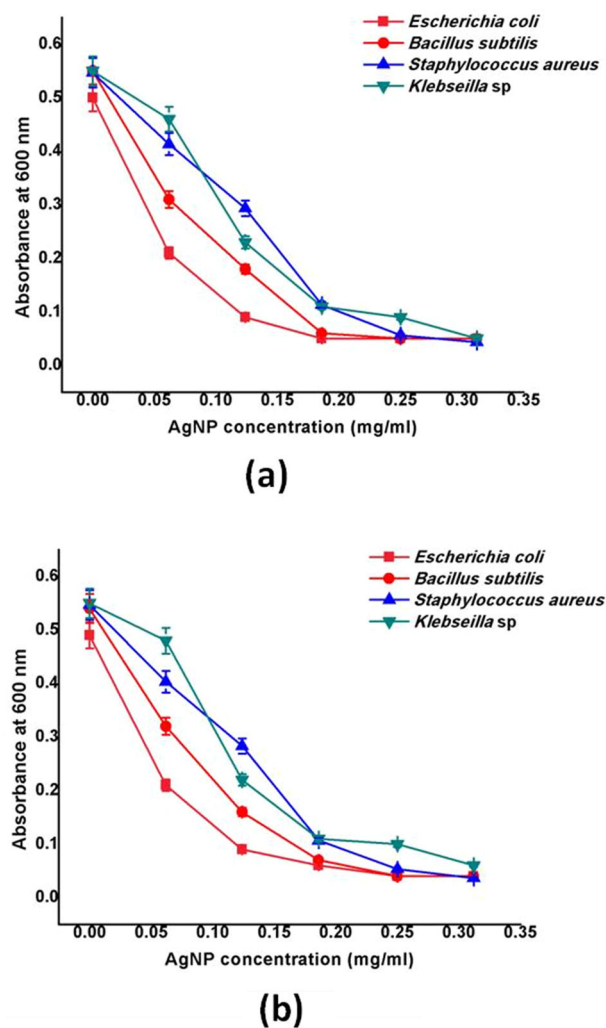


Fig. 5 Bacterial growth curve after treatment with (a) AgNPs from neem leaf extract (b) AgNPs from banana peel extract

Sharma 2012). Wypij et al. (2018) reported the MIC value of AgNPs against *Escherichia coli*, *Bacillus subtilis*, *Staphylococcus aureus*, and *Klebsiella pneumoniae* to be 64, 64, 256, and 256 $\mu\text{g/ml}$ respectively. Chudasama et al. (2010) reported MIC values for silver nanoparticles for different microorganisms. For *Escherichia coli*, *Shigella Sonnei*, *Bacillus megaterium*, *Proteus vulgaris*, and *Staphylococcus aureus* the MIC values were 100 $\mu\text{g/ml}$, 215 $\mu\text{g/ml}$, 275 $\mu\text{g/ml}$, 300 $\mu\text{g/ml}$, and 350 $\mu\text{g/ml}$ respectively. From different studies, it was observed that MIC values for AgNPs synthesized from a variety of sources against different microorganisms were either reported to be high or low. In the present study, it was found that the nanoparticle synthesized from banana peel and neem leaf extract inhibits the growth of the bacteria *Escherichia coli*, *Bacillus subtilis*, *Staphylococcus aureus* at a fixed concentration of 0.25 mg/ml, and in the case of *Klebsiella* the concentration was found to be 0.312 mg/ml. In

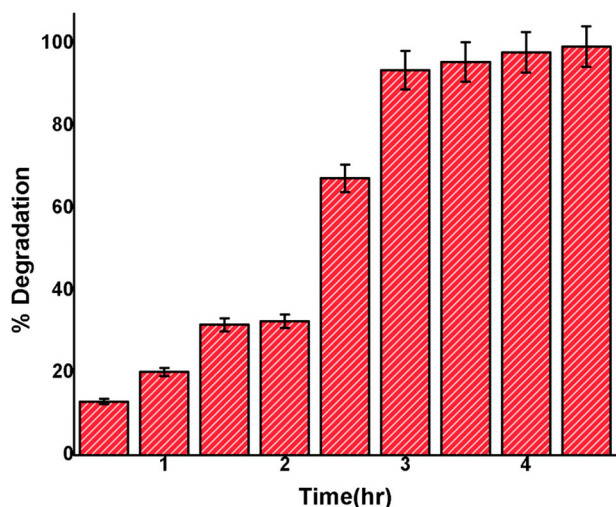


Fig. 6 Time Vs Degradation percentage of malachite green

Supplementary Table 1, 2, 3, 4 MIC analyses for *E.coli*, *B. subtilis*, *S. aureus*, and *Klebsiella* sp. are given respectively.

Photocatalytic degradation of dye

Photocatalytic degradation activity of AgNPs was demonstrated using model dye malachite green. A spectral scan of the samples was performed using a UV-Vis spectrophotometer. A spectral scan of malachite green stock solution showed a peak at 684 nm. The test samples containing different concentrations of AgNPs and dye solution and the control sample (dye solution without AgNPs) were checked for dye degradation. The dye degradation was observed by visualizing the decolorization of the sample and then spectrophotometric analysis. The test sample containing AgNPs at a concentration of 0.06 mg/ml showed decolorization and a decrease in absorption spectra. Further, this test sample was analyzed at an interval of 0.5 h for the same time and experimental conditions to observe the gradual decrease in absorption spectra (Supplementary Fig. 3). No change in the absorption spectra of the control sample was observed. Using standard curve the concentrations were calculated and then using Eq. (1) % degradation was calculated. The calculated values are given in Supplementary Table 5. Degradation percentage against time was plotted and shown in Fig. 6. Poornima and Valivittan (2017) reported the synthesis of AgNPs using red seaweed. They used these biosynthesized nanoparticles to study malachite green dye's degradation and they observed dye degradation within 6 h of incubation. Lakshmi et al. (2016) observed the degradation of malachite green utilizing silver nanoparticles. Within 1 h 45 mins, 69.23% of degradation was observed. In the current study, it was observed that using AgNPs synthesized from banana peel extract a 99% degradation of the model dye was possible within 4.5 h. As

Table 3 % of dye degradation with time

Time (hr)	% Degradation of malachite green
0.5	13.01
1	20.21
1.5	31.65
2	32.5
2.5	67.24
3	93.51
3.5	95.5
4	97.78
4.5	99.2

we have pointed out earlier that from the range of concentration of AgNPs utilized for the degradation, the highest concentration which showed maximum degradation capacity was studied further and the underlying mechanism behind it can be due to the attraction and adsorption of the cationic dye over the surface of the nanoparticles and eventually the degradation of dye by the excited electrons as we have explained earlier (Table 3).

Conclusion

A simple and one-step approach was adapted for synthesizing AgNPs from extract of neem leaves and banana peels which can potentially be used as an antimicrobial and dye degrading agent. This process of synthesis is environment friendly as no chemical agents were used. ESEM analysis revealed that the synthesized AgNPs were spherical. From FTIR analysis it can be concluded that functional groups like aldehyde, alcohol, carboxylic acid, alkane, alkene, and amine participated in AgNPs synthesis. The crystalline nature of the AgNPs was confirmed by the XRD study. DLS studies revealed the average particle size of AgNPs synthesized from banana peel was 168.7 nm with a PDI of 0.394. The zeta potential value was -27 mV. The average particle size of AgNPs synthesized from neem leaf extract was found to be 206.4 nm with a PDI of 0.312. In this case, the zeta potential value was -32.7 mV. Antimicrobial activity of the AgNPs was tested by using the disk diffusion assay against *E.coli*, *B.subtilis*, *S.aureus*, and *Klebsiella* sp. 99% degradation of malachite green was observed after photocatalytic degradation using silver nanoparticles. In this technique, scale-up can be done very easily due to the simplicity of the method. The antimicrobial property of silver nanoparticles has been exploited in various fields, and this property can also be utilized in wastewater treatment. From the study of earlier work, as per our knowledge photocatalytic degradation of malachite green using banana peel derived nanoparticle has not been reported. The

synthesized nanoparticles from banana peels showed that they can be potentially utilized for dye degradation as these nanomaterials were found to be efficient and capable of degrading the dye within a very short period. Thus these particles can be potentially used in the treatment of wastewater.

Compliance with ethical standards

Conflict of interest The authors declare no competing interest.

Publisher's note Springer Nature remains neutral with regard to jurisdictional claims in published maps and institutional affiliations.

References

- Ahmad N, Sharma S (2012) Green synthesis of silver nanoparticles using extracts of *Ananas comosus*. *Green Sustain Chem* 2:141–147
- Ahmed S, Saifullah, Ahmad M, Swami BL, Ikram S (2016) Green synthesis of silver nanoparticles using *Azadirachta indica* aqueous leaf extract. *J Radiat Res Appl Sci* 9:1–7
- Ahmad A, Mukherjee P, Senapati S, Mandal D, Khan MI, Kumar R, Sastry M (2003) Extracellular biosynthesis of silver nanoparticles using the fungus *Fusarium oxysporum*. *Colloids Surf B* 28:313–318
- Agnihotri S, Sillu D, Sharma G, Arya RK (2018) Photocatalytic and antibacterial potential of silver nanoparticles derived from pineapple waste: process optimization and modeling kinetics for dye removal. *Appl Nanosci* 8:2077–2092
- Attar A, Altikatoglu Yapaoz M (2018) Biosynthesis of palladium nanoparticles using *Diospyros kaki* leaf extract and determination of antibacterial efficacy. *Prep Biochem Biotech* 48:629–34
- Awwad AM, Salem NM, Abdeen AO (2013) Green synthesis of silver nanoparticles using carob leaf extract and its antibacterial activity. *Int J Ind Chem* 4:29
- Bankar A, Joshi B, Kumar AR, Zinjarde S (2010) Banana peel extract mediated novel route for the synthesis of silver nanoparticles. *Colloids Surf A Physicochem Eng Asp* 368:58–63
- Banerjee P, Satapathy M, Mukhopahayay A, Das P (2014) Leaf extract mediated green synthesis of silver nanoparticles from widely available Indian plants: synthesis, characterization, antimicrobial property and toxicity analysis. *Bioresour Bioprocess* 1:3
- Chandran SP, Chaudhary M, Pasricha R, Ahmad A, Sastry M (2006) Synthesis of gold nanotriangles and silver nanoparticles using *Aloevera* plant extract. *Biotechnol Prog* 22:577–583
- Chudasama B, Vala AK, Andhariya N, Mehta RV, Upadhyay RV (2010) Highly bacterial resistant silver nanoparticles: synthesis and antibacterial activities. *J Nanopart Res* 12:1677–1685
- Du LN, Wang S, Li G, Wang B, Jia XM, Zhao YH, Chen YL (2011) Biodegradation of malachite green by *Pseudomonas* sp. strain DY1 under aerobic condition: characteristics, degradation products, enzyme analysis and phytotoxicity. *Ecotoxicology* 20:438–446
- Devi TA, Ananthi N, Amaladhas TP (2016) Photobiological synthesis of noble metal nanoparticles using *Hydrocotyle asiatica* and application as catalyst for the photodegradation of cationic dyes. *J Nanostructure Chem* 6:75–92
- Dubey M, Bhadauria S, Kushwaha BS (2009) Green synthesis of nanosilver particles from extract of *Eucalyptus hybrida* (safeda) leaf. *Dig J Nanomater Biostruct* 4:537–543
- Edison TJI, Sethuraman MG (2013) Biogenic robust synthesis of silver nanoparticles using *Punica granatum* peel and its application as a green catalyst for the reduction of an anthropogenic pollutant 4-nitrophenol. *Spectrochim Acta A* 104:262–264
- Esakkimuthu T, Sivakumar D, Akila S (2014) Application of nanoparticles in wastewater treatment. *Pollut Res* 33:567–571
- Francis S, Joseph S, Koshy EP, Mathew B (2017) Green synthesis and characterization of gold and silver nanoparticles using *Mussaenda glabrata* leaf extract and their environmental applications to dye degradation. *Environ Sci Pollut* 24:17347–17357
- Gan L, Zhang S, Zhang Y, He S, Tian Y (2018) Biosynthesis, characterization, and antimicrobial activity of silver nanoparticles by a halotolerant *Bacillus endophyticus* SCU-L. *Prep Biochem Biotech* 48:582–588
- Hameed BH, Lee TW (2009) Degradation of malachite green in aqueous solution by Fenton process. *J Hazard Mater* 164:468–472
- Herlekar M, Barve S, Kumar R (2014) Plant-mediated green synthesis of iron nanoparticles. *J Nanoparticle Res* 2014:1–9
- Hussein E.A.M, Mohammad A.A.H, Harraz F.A, Ahsan M.F (2019) Biologically Synthesized Silver Nanoparticles for Enhancing Tetracycline Activity against *Staphylococcus aureus* and *Klebsiella pneumoniae*. *Braz Arch Biol Technol* 62:e19180266.
- Ibrahim HM (2015) Green synthesis and characterization of silver nanoparticles using banana peel extract and their antimicrobial activity against representative microorganisms. *J Radiat Res Appl Sci* 8:265–275
- Joanna C, Marcin L, Ewa K, Grażyna P (2018) A nonspecific synergistic effect of biogenic silver nanoparticles and biosurfactant towards environmental bacteria and fungi. *Ecotoxicology* 27:352–359
- Jyoti K, Singh A (2016) Green synthesis of nanostructured silver particles and their catalytic application in dye degradation. *J Genetic Eng Biotechnol* 14:311–317
- Kaviya S, Santhanalakshmi J, Viswanathan B, Muthumary J, Srinivasan K (2011) Biosynthesis of silver nanoparticles using *Citrus sinensis* peel extract and its antibacterial activity. *Spectrochim Acta A* 79:594–598
- Khalil MM, Ismail EH, El-Baghdady KZ, Mohamed D (2014) Green synthesis of silver nanoparticles using olive leaf extract and its antibacterial activity. *Arab J Chem* 7:1131–1139
- Kokila T, Ramesh PS, Geetha D (2015) Biosynthesis of silver nanoparticles from Cavendish banana peel extract and its antibacterial and free radical scavenging assay: a novel biological approach. *Appl Nanosci* 5:911–920
- Kumar V, Yadav SC, Yadav SK (2010) *Syzygium cumini* leaf and seed extract mediated biosynthesis of silver nanoparticles and their characterization. *J Chem Technol Biot* 85:1301–1309
- Kumari RM, Thapa N, Gupta N, Kumar A, Nimesh S (2016) Antibacterial and photocatalytic degradation efficacy of silver nanoparticles biosynthesized using *Cordia dichotoma* leaf extract. *Adv Nat Sci-nanosci* 7:045009
- Lakshmi SP, Dhanya S, Sheeba D (2016) Photocatalytic degradation of malachite green using silver nanoparticles synthesised from gooseberry extract. *J Chem Mater Res* 5:68–73
- Loo YY, Rukayadi Y, Nor-Khaizura MA, Kuan CH, Chieng BW, Nishibuchi M, Radu S (2018) In vitro antimicrobial activity of green synthesized silver nanoparticles against selected gram-negative foodborne pathogens. *Front Microbiol* 9:1555
- Mariselvam R, Ranjitsingh AJA, Nanthini AUR, Kalirajan K, Padmalatha C, Selvakumar PM (2014) Green synthesis of silver nanoparticles from the extract of the inflorescence of *Cocos nucifera* (Family: Arecaceae) for enhanced antibacterial activity. *Spectrochim Acta A* 129:537–541
- Mallikarjuna K, Narasimha G, Dillip GR, Praveen B, Shreedhar B, Lakshmi CS, Reddy BVS, Raju BDP (2011) Green synthesis of silver nanoparticles using *Ocimum* leaf extract and their characterization. *Dig J Nanomater Bios* 6:181–186

- Nakkala JR, Mata R, Gupta AK, Sadras SR (2014) Biological activities of green silver nanoparticles synthesized with *Acorous calamus* rhizome extract. *Eur J Med Chem* 85:784–794
- Poornima S, Valivittan K (2017) Degradation of malachite green (dye) by using photo-catalytic biogenic silver nanoparticles synthesized using red algae (*Gracilaria corticata*) aqueous extract. *Int J Curr Microbiol Appl Sci* 6:62–70
- Rautela A, Rani J, Das MD (2019) Green synthesis of silver nanoparticles from *Tectona grandis* seeds extract: characterization and mechanism of antimicrobial action on different microorganisms. *J Anal Sci Technol* 10:1–10
- Samanta HS, Das R, Bhattachajee C (2016) Influence of nanoparticles for wastewater treatment—a short review. *Austin Chem Eng* 3:1036
- Shanmugavadivu M, Kuppusamy S, Ranjithkumar R (2014) Synthesis of pomegranate peel extract mediated silver nanoparticles and its antibacterial activity. *Am J Adv Drug Deliv* 2:174–182
- Singh A, Jain D, Upadhyay MK, Khandelwal N, Verma HN (2010) Green synthesis of silver nanoparticles using *Argemone mexicana* leaf extract and evaluation of their antimicrobial activities. *Dig J Nanomater Bios* 5:483–489
- Tripathi A, Chandrasekaran N, Raichur AM, Mukherjee A (2009) Antibacterial applications of silver nanoparticles synthesized by aqueous extract of *Azadirachta indica* (Neem) leaves. *J Biomed Nanotechnol* 5:93–98
- Varadavenkatesan T, Selvaraj R, Vinayagam R (2019) Dye degradation and antibacterial activity of green synthesized silver nanoparticles using *Ipomoea digitata* Linn. flower extract. *Int J Environ Sci Te* 16:2395–2404
- Vidhu VK, Philip D (2014) Catalytic degradation of organic dyes using biosynthesized silver nanoparticles. *Micron* 56:54–62
- Verma A, Mehata MS (2016) Controllable synthesis of silver nanoparticles using Neem leaves and their antimicrobial activity. *J Radiat Res Appl Sci* 9:109–115
- Wei X, Zhou H, Xu L, Luo M, Liu H (2014) Sunlight-induced biosynthesis of silver nanoparticles by animal and fungus biomass and their characterization. *J Chem Technol Biot* 89:305–311
- Wypij M, Czarnicka J, Świecimska M, Dahm H, Rai M, Golinska P (2018) Synthesis, characterization and evaluation of antimicrobial and cytotoxic activities of biogenic silver nanoparticles synthesized from *Streptomyces xinghaiensis* OF1 strain. *World J Microb Biot* 34:23
- Yurtluk T, Akçay FA, Avci A (2018) Biosynthesis of silver nanoparticles using novel *Bacillus* sp. SBT8. *Prep Biochem Biotech* 48:151–159